*Acta Cryst.* (1950). **3**, 236

# Diffraction by Cylindrical Bodies with Periodic Axial Structure†

By Richard S. Bear and Orvil E. A. Bolduan‡

*Department of Biology, Massachusetts Institute of Technology, Cambridge, Massachusetts, U.S.A.*

(*Received* 12 *September* 1949)

The diffractions expected of representative cylindrical bodies with periodic axial density variations, but lacking regular order over cross sections, are calculated herein. Three models are considered: (1) the *smooth* cylinder, whose radius is everywhere constant; (2) the *corrugated* cylinder, whose radius is a periodic function of position along the cylinder with the same period as the axial density variations; and (3) the *compound* cylinder, which is composed of thin, parallel, smooth cylinders displaced axially from perfect transverse matching of their identical axial density fluctuations.

These models are readily distinguished by the characteristic ways in which their reciprocal-array disk diameters depend upon layer-line index: with the smooth cylinder disk diameter is independent of index; with the corrugated diffractor diameters at different layer lines vary about a mean value; while with the compound model the diameters progressively enlarge with increasing index. These relations are of particular interest in connection with studies of the small-angle diffraction of collagen fibrils.

## Introduction

A number of the effects exhibited by the fibrous protein collagen at small diffraction angles suggest that the constituent ultramicroscopic fibrils are order-deficient structures possessing unidirectional (axial) periodic variations in density (Bolduan & Bear, 1950). In order to facilitate more searching examination of the fibrillar organization the present discussion considers the diffraction problems offered by certain cylindrical models believed likely to bear some relation to the observed phenomena.

The diffraction problems herein considered possess a certain amount of general interest, since few cases involving cylindrical distribution of matter have been described. Wrinch (1946) derived the Fourier transform of an assemblage of atoms with rotational symmetry about an axis, but not one in which periodic repetition of structure occurs along the axis. MacGillavry & Bruins (1948) presented the Patterson transforms generally applicable to fiber or rotation diagrams. Neither of these formulations is directly useful for the present purposes.

A recent general discussion of the diffraction phenomena accompanying deficiency of order in fibrous systems (Bear & Bolduan, 1950) pointed out the value of familiarity with the properties of the disks representing one-dimensionally ordered structures in reciprocal space. The results obtained below contribute to an understanding of the significance of such phenomena as variations in disk diameter with index, which are actually encountered with collagen specimens.

† This paper represents a partial report on research sponsored by the Office of the Quartermaster General, Research and Development Branch, under Project no. 130–46 on 'Determination of the Nature and Properties of Skin Structure', under direction of the Leather Subcommittee of the National Research Council Committee on Quartermaster Problems.

‡ Present address: Camp Detrick, Frederick, Maryland, U.S.A.

## The smooth-cylinder model

The starting point is a treatment of the simplest possible model consistent with the gross structure features of collagen fibrils as recognized from electron-microscope and small-angle diffraction studies. This involves determination of the diffraction expected of a cylinder of length $L$ and radius $R$. Electron-density variations repeat many times, every $b_0$ distance, in the direction of the cylinder axis ($y$), but at any given level the density is considered to be uniform over the entire cross section of the fibril. Since the radius is constant at all levels, this particular model may be termed briefly the 'smooth cylinder' model. While this could be developed as a special case of Wrinch's rotation-symmetrical system, it is desirable to outline the complete treatment in order to facilitate subsequent consideration of more complex situations.

In Fig. 1 the unit vector $\mathbf{s}_0$ ($CO$) represents the direction of an X-ray beam incident at the angle $\theta$ to the cylinder normal, which is drawn at $C$ near one end of the fibril in the plane determined by the cylinder axis and $\mathbf{s}_0$. The unit vector $\mathbf{s}$ ($CP$) extends toward $P$, the point at which diffracted intensity is to be registered. Locations in the cyinder are specified by the vector $\boldsymbol{\rho}$ whose cylindrical co-ordinates $r$, $\psi$ and $y$ are stated with reference to the co-ordinate axes of the cylinder. At $O$ is located the origin of reciprocal space, whose vector $\boldsymbol{\rho}^* = \mathbf{s} - \mathbf{s}_0$ has also cylindrical components $r^*$, $\psi^*$ and $y^*$, referred to axes which remain parallel to the corresponding ones of the original diffracting cylinder. The sphere swept out by the possible positions for the

vector **s** is the *sphere* of reflection, which for small angles of diffraction becomes a *plane* of reflection normal to $\mathbf{s}_0$ at $O$ (cf. Bear & Bolduan, 1950).

As is well known from diffraction theory,† the intensity of radiation of wave-length $\lambda$, scattered toward the end of the vector $\rho^*$ in the plane of reflection, is

$$I_{\rho^*} = I_0 i_e \left| \int N(\rho) \exp\left[i2\pi\tilde{\nu}(\rho \cdot \rho^*)\right] d\tau \right|^2,$$

where $I_0$ is the intensity of the beam incident at $C$; $i_e$ is the intensity scattered by a single electron for unit incident intensity, being at small diffraction angles a function solely of certain universal physical constants; $N(\rho)$ is the density of electrons in the element of cylinder volume $d\tau$ located at the end of $\rho$; and $\tilde{\nu}$ is the reciprocal of $\lambda$, the wave-length being scattered. Integration is over the entire volume of the cylinder.

where $J_0$ is the usual Bessel function of zero order. The integration with respect to $r$ is then

$$2\pi \int_0^R r J_0(2\pi\tilde{\nu} r r^*)\, dr = \pi R^2 \cdot \frac{J_1(2\pi\tilde{\nu} R r^*)}{\pi\tilde{\nu} R r^*}.$$

The integration along the $y$ axis is carried out according to standard practise by breaking the total cylinder length, $L$, into the number, $M$, of segments, each of length $b_0$, over which $N(y)$ repeats ($M = L/b_0$). This leads eventually to the intensity expression:

$$I_{\rho^*} = I_0 i_e (\pi R^2)^2 \left[\frac{J_1(2\pi\tilde{\nu} R r^*)}{\pi\tilde{\nu} R r^*}\right]^2 \frac{\sin^2(\pi\tilde{\nu} M b_0 y^*)}{\sin^2(\pi\tilde{\nu} b_0 y^*)} |F|^2,$$

where $$F = \int_0^{b_0} N(y) \exp(i2\pi\tilde{\nu} y y^*)\, dy,$$

which may be said to be the *fibril density structure factor*.

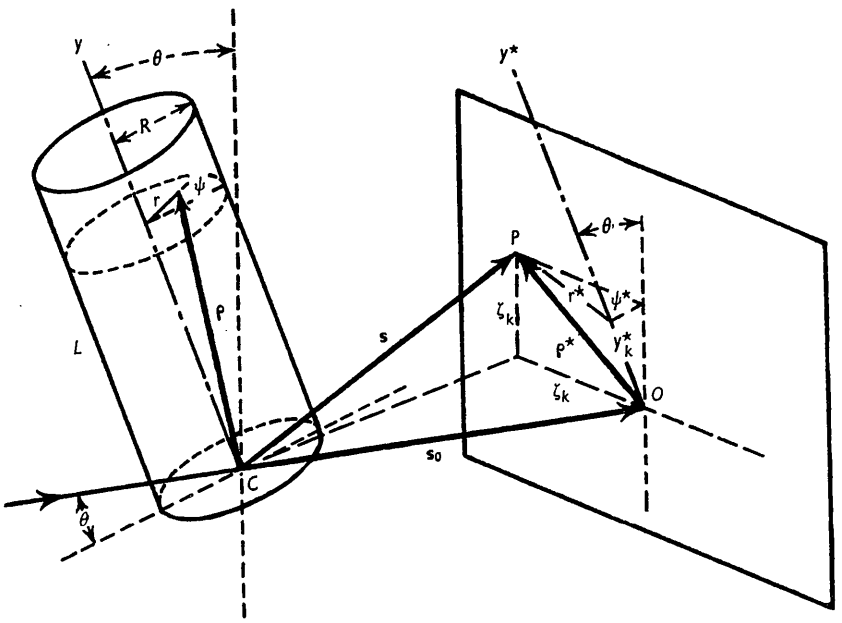


Fig. 1. Construction for the problem of the diffraction by a smooth cylinder. The symbols are explained in the text.

It is readily shown that the scalar product

$$\rho \cdot \rho^* = r r^* \cos(\psi - \psi^*) + y y^*.$$

Also, in the smooth-cylinder model electron density is to be a function only of $y$. Consequently the volume integral becomes

$$\int_0^L N(y) \exp(i2\pi\tilde{\nu} y y^*)\, dy \times \int_0^R \int_0^{2\pi} r \exp\left[i2\pi\tilde{\nu} r r^* \cos(\psi - \psi^*)\right] dr\, d\psi.$$

Since integration over $\psi$ involves a complete cycle, the result is independent of $\psi^*$ and yields $2\pi J_0(2\pi\tilde{\nu} r r^*)$,

† A number of the results of physical and mathematical theory are assumed herein. Relative to the diffraction theory, see, for example, Wrinch (1946) and James (1948). The integrals leading to or involving Bessel functions are discussed in standard works, such as Watson (1944).

This intensity function is rotationally symmetrical about the $Oy^*$ axis of reciprocal space, since $\psi^*$ does not appear. Maxima occur along the $y^*$ axis at $y_k^* = k\lambda/b_0$, where $k$ is an integer (diffraction order index) specifying each maximum. The reciprocal-space representation of the diffraction by the cylinder is, consequently, a series of 'disks' which may be moved through the plane of reflection by tilting the specimen.

In most fiber problems the number $M$ of unit segments, coherently contributing to each disk and constituting the effective diffracting length of the cylinder, is large. Consequently, the term

$$\sin^2(\pi\tilde{\nu} M b_0 y^*)/\sin^2(\pi\tilde{\nu} b_0 y^*)$$

concentrates the intensity sharply near the central plane of each disk at $y_k^*$. Over the range of $y^*$ at which

this term has appreciable value, the structure factor remains practically constant at

$$F_k=\int_0^1 N(v)\exp(i2\pi kv)\,dv,$$

where $v$ is a co-ordinate of longitudinal position in the original cylinder, expressed now in fractions of the period $b_0$.

One may define a 'thickness' for each disk as being the distance along $Oy^*$ between planes of constant $y^*$ at which the intensity of the disk (for any $r^*$) falls to half its value at the maximum central plane. In order to determine this, one may make the transformation $y^*=y^*+\epsilon$, in which $\epsilon$ is a small departure from the $y_k^*$ at which maximum intensity occurs. Under these conditions $\sin^2(\pi\tilde{\nu}Mb_0y^*)=\sin^2(\pi\tilde{\nu}Mb_0\epsilon)$

and $\sin^2(\pi\tilde{\nu}b_0y^*)\doteq(\pi\tilde{\nu}b_0\epsilon)^2$.

Since on the central plane of the disk (at $\epsilon=0$)

$$\sin^2(\pi\tilde{\nu}Mb_0\epsilon)/(\pi\tilde{\nu}b_0\epsilon)^2=M^2,$$

a 'shape factor' for distribution of intensity along $Oy^*$ *relative* to that at the central plane is

$$S_{k\epsilon}=\frac{\sin^2(\pi\tilde{\nu}Mb_0\epsilon)}{(\pi\tilde{\nu}Mb_0\epsilon)^2}\doteq\exp[-(\pi\tilde{\nu}Mb_0\epsilon)^2/\pi].$$

The exponential approximation is well known to be good for shape of an $S_{k\epsilon}:\epsilon$ plot and is exact for the area under such a curve. It is particularly convenient for practical applications, as is seen in the present one wherein the thickness of the disk as defined above becomes easily expressed as

$$\{2\sqrt{(-\pi\ln 0{\cdot}5)}\}/\pi\tilde{\nu}Mb_0.$$

Note that disk thickness is independent of $k$, which is a consequence of the fact that structure was assumed to possess perfect periodicity along the cylinder axis. Any distortions from perfect repetition of segments would tend to make the effective number of segments contributing coherent scatter to the various disks depend on index, so that disk *thickness* would be variable. In actual fact, however, practical fibrous diffractors exhibit such large $M$'s for all disks that at small diffraction angles resolution of line shape along pattern meridians is rarely accomplished. Under such conditions it is convenient to deal with disks whose intensity has been collapsed by projection on to their central planes. These may be termed *integrated intensity disks*, and expressions for them may be immediately written after noting that

$$M^2\int_{-\infty}^{+\infty}S_{k\epsilon}d\epsilon=\frac{M\lambda}{b_0}$$

is the factor which must replace

$$\sin^2(\pi\tilde{\nu}Mb_0y^*)/\sin^2(\pi\tilde{\nu}b_0y^*)$$

in $I_{\rho^*}$. Consequently, the intensity per unit area of the integrated $k$th disk is

$$I_{kr^*}=\frac{I_0i_eM\lambda}{b_0}(\pi R^2)^2\left[\frac{J_1(2\pi\tilde{\nu}Rr^*)}{\pi\tilde{\nu}Rr^*}\right]^2|F_k|^2. \qquad (1)$$

As in considering disk thickness, one may also define a 'diameter' as the distance across a disk (through the center) between radial points at which a shape factor has fallen to half its central value. The radial shape factor in this case is

$$S_{kr^*}=\left[\frac{J_1(2\pi\tilde{\nu}Rr^*)}{\pi\tilde{\nu}Rr^*}\right]^2\doteq\exp[-(\pi\tilde{\nu}Rr^*)^2], \qquad (2)$$

expressing the intensity at a radial position $r^*$ *relative* to that at the disk center. The exponential approximation is perfect for shape at small $r^*$, reasonable for general trend over all $r^*$, and good for area under an $S_{kr^*}$, $r^*$ plot, as can be readily shown graphically. The exponential approximation permits the expression of disk diameter as $\{2\sqrt{(-\ln 0{\cdot}5)}\}/\pi\tilde{\nu}R$.

As with thickness, the disk diameter is independent of index, corresponding to the fact that the smooth-cylinder model assumes constant radius at all $y$ levels of the cylinder for coherent scatter to all disks. The disk diameter will not remain independent of $k$, however, if this constancy of diffractor radius is disturbed. The following models illustrate this fact for other structures which may also be described as one-dimensionally ordered, and which have been chosen to show in as simple fashion as possible two distinct ways in which effective diffractor radii may be altered from the smooth cylinder case.

### The corrugated cylinder

The simplest deviation from the smooth-cylinder model, which also seems of interest with respect to known facts regarding collagen fibril structure, is one introducing the periodic diametral depressions and elevations that can be seen in electron micrographs (see Schmitt & Gross, 1948). This 'corrugated' cylinder, whose radius variations are closely related to the periodic axial density fluctuations, is shown diagrammatically in Fig. 2 (*b*).

Determination of the diffraction by the corrugated cylinder is differentiated from the corresponding smooth-cylinder considerations by the circumstance that the radius at any $y$ level of the fibril is a function of that level. Consequently, at the stage of integration over cylinder length one finds the intensity expression:

$$I'_{\rho^*}=I_0i_e\frac{\sin^2(\pi\tilde{\nu}Mb_0y^*)}{\sin^2(\pi\tilde{\nu}b_0y^*)}|F'|^2,$$

where $F'$, the total structure factor for the unit of pattern of the corrugated cylinder, is

$$\int_0^{b_0}\pi R_y^2\frac{J_1(2\pi\tilde{\nu}R_yr^*)}{\pi\tilde{\nu}R_yr^*}N(y)\exp(i2\pi\tilde{\nu}yy^*)\,dy,$$

the $y$ subscript on $R$ indicating the dependence of radius on level.

The cases to which the model need be applied, judging from most existing electron micrographs, are those in which the departures of $R_y$ from some average radius, $R$, are small. Consequently, if $R_y=R+\Delta R_y$, where

$\Delta R_y$ is the small positive or negative deviation in fibril radius, expansion by Taylor's series of the terms of the above integrand which are functions of $R_y$ yields

$$\pi R_y^2 \frac{J_1(2\pi\tilde{\nu}R_y r^*)}{\pi\tilde{\nu}R_y r^*} \doteqdot \pi R^2\left[\frac{J_1(2\pi\tilde{\nu}Rr^*)}{\pi\tilde{\nu}Rr^*} + J_0(2\pi\tilde{\nu}Rr^*)\frac{\Delta R_y}{R}\right]$$

to the approximation which neglects all powers of $\Delta R_y/R$ higher than the first. Substitution of this into the total structure factor, plus some simple rearrangement, produces

$$F' \doteqdot \pi R^2\left[\frac{J_1(2\pi\tilde{\nu}Rr^*)}{\pi\tilde{\nu}Rr^*} F + J_0(2\pi\tilde{\nu}Rr^*)\, G\right],$$

in which $F$ is essentially the previous structure factor of the smooth-cylinder case, while $G$ is a new one which carries largely the effects of the radius variations. When the $y^*$ positions for maximum intensity are noted to be the same as for the smooth cylinder, it becomes possible to express $G$ as follows:

$$G_k = \int_0^1 N(v)\frac{\Delta R_v}{R}\exp(i2\pi kv)\,dv,$$

which may be called the *radius* structure factor to distinguish it from the previously defined *density* structure factor, $F_k$.

Other considerations regarding the corrugated cylinder are similar to those developed for the smooth cylinder. The final integrated intensity disk is found to have intensity spread over it according to

$$I'_{kr^*} = \frac{I_0 i_e M\lambda}{b_0}(\pi R^2)^2\left|\frac{J_1(2\pi\tilde{\nu}Rr^*)}{\pi\tilde{\nu}Rr^*} F_k + J_0(2\pi\tilde{\nu}Rr^*)\, G_k\right|^2. \tag{3}$$

Equation (3) indicates that the disks of the corrugated cylinder may possess a variety of shapes ranging from that of a smooth cylinder (when $|F_k| \gg |G_k|$) to that caused largely by the radius variations (when $|F_k| \ll |G_k|$). In the latter case the shape of $J_0^2(2\pi\tilde{\nu}Rr^*)$ is expected, in which there is a central maximum on the meridian and lesser lateral maxima to either side, the most prominent of which would be at $\pi\tilde{\nu}Rr^* = 1{\cdot}9$. Although, because of complex structure of corrugated-cylinder disks, the concept of diameter for these may have no simple meaning, one notes that the extent of disk over which major intensity can be spread is limited in the same way for all disks. Whether major intensity is applied close to or is somewhat spread from the meridional center depends on incidents of structure effective in determining the relative importances of the structure factors $F_k$ and $G_k$.

It is useful to consider, as a special case of the corrugated cylinder, one in which the radius variations furnish small perturbations on the diffraction effects of a nearly smooth cylinder, i.e. a situation in which generally $|G_k| < |F_k|$, but the radius structure factor is not negligible. It is readily shown that

$$S'_{kr^*} = \left[\frac{2J_1(\alpha)}{\alpha}\right]^2\left\{1 + 4c_k\frac{[J_0(\alpha) - 2J_1(\alpha)/\alpha]}{2J_1(\alpha)/\alpha}\right\}$$

is the radial shape function for the disks of the 'slightly corrugated' cylinder, where $\alpha$ is the common argument $(2\pi\tilde{\nu}Rr^*)$ of the Bessel functions, and

$$2c_k = (g/f)\cos(\omega_g - \omega_f),$$

$g$ and $f$ being the amplitudes, and $\omega_g$ and $\omega_f$ the phases, of the structure factors $G_k$ and $F_k$ respectively. In the approximations involved, $c_k$ is considered small compared to unity and may be either positive or negative depending on the structure-factor phases.

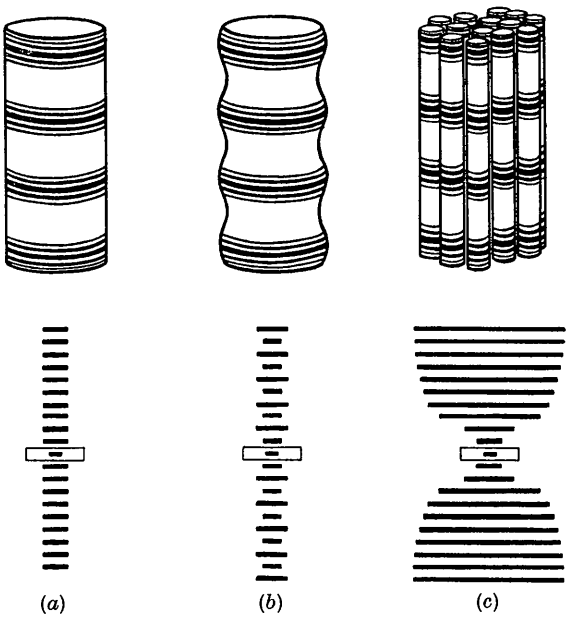


Fig. 2. Diagrammatic representations of the three cylindrical models (above) with their characteristic layer-line length variations (below): (*a*) for the smooth cylinder, (*b*) for the slightly corrugated cylinder, and (*c*) for the compound cylinder. In actual pinhole diffraction patterns these simple length relationships may be disguised somewhat by the varying intensities of layer lines produced by incidental structure-factor influences. The alternation of line lengths shown for the corrugated cylinder is only one of the possible ways that lengths may vary about a mean.

At small $\alpha$,

$$[J_0(\alpha) - 2J_1(\alpha)/\alpha]/[2J_1(\alpha)/\alpha] \doteqdot \alpha^2/8,$$

and the following power-series approximation for the second factor of $S'_{kr^*}$ may be used:

$$1 + (c_k\alpha^2/2) = \exp(c_k\alpha^2/2).$$

It is thus possible to formulate a rough shape function for the slightly corrugated cylinder:

$$S'_{kr^*} = \exp[-(\pi\tilde{\nu}Rr^*)^2(1 - 2c_k)], \tag{4}$$

in which the same exponential approximation for $[2J_1(\alpha)/\alpha]^2$ has been employed as with the smooth cylinder.

Comparison of this result with equation (2) shows that, since the $c_k$'s may be either positive or negative, the various diameters of different disks in the corrugated cylinder case will fluctuate above and below the constant value expected of a smooth cylinder of the same average radius.

### The compound cylindrical fibril

A totally different way in which cylinder cross sections for coherent diffraction may be altered is encountered with a model in which the previous smooth cylinder is imagined to be divided into thin columnar elements (the subfibrillar 'filaments' of Schmitt & Gross (1948)) which are displaced axially out of perfect register across cylinder cross sections. Electron-microscope evidence for longitudinal cleavage of collagen fibrils and their dispersion into filaments by acetic acid lends support to the possibility of this general type of structure.

To consider initially the simplest model of a compound cylindrical fibril it will be supposed to be made of many identical filaments in near register. The departures from perfect matching between filaments are supposed to be due to random minor displacements of the filaments as wholes in the direction of the fibril axis (see Fig. 2 (*c*)). The total cylinder is of radius $R$ as before, while each filament has a radius $R_0$. It is also supposed that $R_0$ is much smaller than $R$, so that one may speak of a nearly uniform distribution of filaments in any fibril cross section.

Each filament, if independent of others, would diffract according to the smooth-cylinder equations developed previously. It is necessary, however, to take account of phase relations of the scattering by different filaments. This is done in the structure factor of the following equation:

$$I''_{kr^*}=I_{0kr^*}\,|\,F''_{kr^*}\,|^2,$$

where $I''_{kr^*}$ is the integrated disk intensity for the compound fibril, $I_{0kr^*}$ that given above (equation (1) with $R_0$ in place of $R$) for a single smooth cylindrical filament, and $F''_{kr^*}$ is a structure factor taking account of the number and the arrangement of filaments relative to one another.

For the sake of brevity the structure factor $F''_{kr^*}$ will not be derived here. Actually, because the axial displacement of filaments is statistical, only an average value of $|\,F''_{kr^*}\,|^2$ can be calculated. This will be determined on another occasion in connection with a more general model for a distorted compound fibril, of which the present one is a special case chosen for consideration here because of its simple relation to the smooth cylinder.

It is found that

$$\overline{|\,F''_{kr^*}\,|^2}=\frac{\pi R^2(k\pi\sigma_b/b_0)^2}{2\pi R_0^2[(k\pi\sigma_b/b_0)^4+(\pi\tilde{\nu}R_0r^*)^2]^{\frac{3}{2}}},$$

where $\sigma_b$ is a small displacement (root of the mean square value) introduced at random along positive or negative axial directions as one passes across the fibril from any one filament to any next neighbor. The correctness of this formulation will be apparent, qualitatively at least, from the physical reasonableness of the results attained below for the effective diffractor radii of the compound fibril.

It follows that the average intensity of the integrated disk is

$$\overline{I''_{kr^*}}=\frac{I_0 i_e M\lambda\pi R^2\pi R_0^2(k\pi\sigma_b/b_0)^2}{2b_0[(k\pi\sigma_b/b_0)^4+(\pi\tilde{\nu}R_0r^*)^2]^{\frac{3}{2}}}\times\left[\frac{J_1(2\pi\tilde{\nu}R_0r^*)}{\pi\tilde{\nu}R_0r^*}\right]^2|\,F_k\,|^2 \quad (5)$$

for the compound fibril. From this the radial shape factor is readily shown to be

$$S''_{kr^*}=\left[1+\frac{(\pi\tilde{\nu}R_0r^*)^2}{(k\pi\sigma_b/b_0)^4}\right]^{-\frac{3}{2}}\left[\frac{J_1(2\pi\tilde{\nu}R_0r^*)}{\pi\tilde{\nu}R_0r^*}\right]^2.$$

It is convenient to employ the approximate exponential form $\exp[-C(\pi\tilde{\nu}R_0r^*)^2/(k\pi\sigma_b/b_0)^4]$ for the first factor of this expression, where the approximation for shape is perfect at small $r^*$ when $C=1{\cdot}5$, or perfect for area (under a curve in which this factor is plotted as ordinate against $r^*$ as abscissa) when $C=\frac{1}{4}\pi$. With exponential approximation employed also for the Bessel-function factor, one then finds

$$S''_{kr^*}=\exp\left\{-(\pi\tilde{\nu}R_0r^*)^2\left[1+\frac{C}{(k\pi\sigma_b/b_0)^4}\right]\right\}. \quad (6)$$

This equation readily discloses that disk diameters expand with increase in $k$ (see further below).

### Conclusion

While the above development has occasionally neglected minor details of disk shape, the exponential functions of equations (2), (4) and (6) are sufficiently reliable for many purposes, serving as guides to the general influence of pertinent parameters on reciprocal-array disk shapes.

The discussion to this point has emphasized disk diameters and their variation with index. In practical work one is more interested in obtaining information regarding the actual diffracting structure. It now becomes possible to transfer attention to certain effective diffractor radii which are reciprocally related to the disk diameters.

Study of equations (2), (4) and (6) shows that they all have the common form

$$S_{kr^*}=\exp[-(\pi\tilde{\nu}R_kr^*)^2]. \quad (7)$$

They are distinguished by possessing different expressions for the quantity $R_k$, as follows:

$R_k=R$ (smooth cylinder),

$R'_k=R\sqrt{(1-2c_k)}\doteqdot R(1-c_k)$ (slightly corrugated cylinder),

$$R''_k=\frac{R_0\sqrt{\{C+(k\pi\sigma_b/b_0)^4\}}}{(k\pi\sigma_b/b_0)^2}$$ (compound cylinder).

From the fact that $R_k$ in the smooth-cylinder case is directly the radius of the diffractor, it is suggested that $R_k$ should be regarded in all cases as the *effective* radius of the diffractor for its $k$th disk.

Physically this is reasonable. In the corrugated cylinder the effective radius varies about the average

cylinder radius, $R$, because of the positive and negative values possible for the $c_k$ parameters of structure. In the compound cylinder case, when $k$ (or the product $k\sigma_b$) is sufficiently large $R''_k$ approaches $R_0$, in which case individual filaments are essentially diffracting independently. One must keep in mind, however, that as $k\sigma_b$ approaches zero, leading essentially back to the smooth cylinder case, $R''_k$ should approach the relatively large value $R$ but not become infinitely large as given by the equation. This difficulty is a result of an excessive upper limit ($\infty$) assigned during a radial integration in the evaluation of $\overline{|F''_{kr*}|^2}$ but is easily avoided in practical cases by restricting application to layer lines of high index.

$R_k$ can be used generally wherever $R$ occurs in the theory for the particular case of the smooth cylinder, with restriction required, however, to applications involving reciprocal-array disk shapes and dimensions. For example, disk diameters are generally calculable from $\{2\sqrt{(-\ln 0{\cdot}5)}/\pi\bar{\nu}R_k\}$, which was derived above only for the smooth cylinder. On the other hand, $R_k$ substituted for $R$ everywhere in equation (1) does not lead to appropriate approximations of equations (3) and (5).

In actual studies one obtains experimental shape functions for a given specimen as follows: A given point of the $k$th disk is brought into the plane of reflection by a tilt $\theta$ to a position whose co-ordinates in the reflection plane are $\xi$ and $\zeta_k$. As is apparent from Fig. 1,

$$\zeta_k = y^*_k/\cos\theta.$$

Also $y^{*2}_k + r^{*2} = \xi^2 + \zeta^2_k$, from which it follows, since $y^*_k = k\lambda/b_0$, that

$$r^* = \sqrt{\{\xi^2 + (k\lambda/b_0)^2 \tan^2\theta\}}.$$

When this value of $r^*$ is used in equation (7), one obtains the expression (useful under pinhole-camera conditions) indicating the way in which at a given tilt, $\theta$, intensity should vary along the $k$th layer line as a function of $\xi$, the angular departure from the meridional line. On the other hand, one may examine how intensity at constant $\xi$ on a given line depends upon tilt. The former application deals with 'line shape', the latter with 'persistence of intensity with tilt'. This program is an ideal one; actual methods will be detailed elsewhere in connection with a presentation of results of collagen studies.

As illustration of phenomena to be expected of the three types of diffractor under consideration, Fig. 2 indicates diagrammatically the diffraction patterns expected of them under the condition of zero tilt. Only relative line lengths, corresponding to intersections of disk diameters with the reflection plane, are shown. The distinctively different characters of these patterns suggest that the models should be readily recognizable when encountered. In actual cases one sometimes finds combinations of these diffraction effects, but study of the observed line lengths (and similar quantities) in relation to these simple theoretical cases can suggest means for arriving at a model tailored to fit the diffractor at hand.

### References


BEAR, R. S. & BOLDUAN, O. E. A. (1950). *Acta Cryst.* **3**, 230.

BOLDUAN, O. E. A. & BEAR, R. S. (1950). *J. Polym. Sci.* (in press).

JAMES, R. W. (1948). *The Optical Principles of the Diffraction of X-Rays*. London: Bell.

MACGILLAVRY, C. H. & BRUINS, E. M. (1948). *Acta Cryst.* **1**, 156.

SCHMITT, F. O. & GROSS, J. (1948). *J. Amer. Leath. Chem. Ass.* **43**, 658.

WATSON, G. N. (1944). *Theory of Bessel Functions*. Cambridge: University Press.

WRINCH, D. (1946). *Fourier Transforms and Structure Factors*. Cambridge, Mass: Murray.


## Short Communications

*Contributions intended for publication under this heading should be expressly so marked; they should not exceed about 500 words; they should be forwarded in the usual way to the appropriate Co-editor; they will be published as speedily as possible; and proofs will not generally be submitted to authors. Publication will be quicker if the contributions are without illustrations.*

*Acta Cryst.* (1950). **3**, 241

**The diffuse scattering of $NaClO_3$.** By M. S. AHMED and K. LONSDALE, *Chemistry Department, University College, Gower Street, London W.C. 1, England.*

(*Received* 3 *November* 1949)

In a recent paper (Garrido, 1948*a*; published in full in the *Memorias de la Real Academia de ciencias exactas de Madrid* (Garrido, 1948*b*)) the diffuse scattering regions surrounding the reciprocal-lattice points of $NaClO_3$ are deduced from a series of Laue photographs, and are alleged to show long protuberances along two cube-axis directions, resulting in a square cross.

Sen (1949) has pointed out that these results conflict with calculations from the thermal vibration theory, and infers that the theory is thereby disproved.

Ramachandran & Wooster (1950) have, however, repeated the measurements of diffuse scattering, for selected sections of reciprocal space, using the Geiger-counter method and very perfect $NaClO_3$ crystals; and